Magnetic anisotropy of single-crystalline UNi2Al3

Suellow, S.; Becker, B.; de Visser, A.; Mihalik, M.; Nieuwenhuys, G.J.; Menovsky, A.A.; Mydosh, J.A.

DOI
10.1088/0953-8984/9/4/011

Publication date
1997

Published in
Journal of Physics-Condensed Matter

J. Phys.: Condens. Matter **9** (1997) 913–922. Printed in the UK PII: S0953-8984(97)76593-7

Magnetic anisotropy of single-crystalline UNi_2Al_3

S Süllow†, B Becker†, A de Visser‡, M Mihalik‡, G J Nieuwenhuys†, A A Menovsky†‡ and J A Mydosh†

† Kamerlingh Onnes Laboratory, 2300 RA Leiden, The Netherlands
‡ Van der Waals–Zeeman Laboratory, 1018 XE Amsterdam, The Netherlands

Received 24 July 1996, in final form 30 September 1996

Abstract. We report the magnetic field dependence of the dc susceptibility and resistivity in superconducting single crystals of the hexagonal heavy-fermion superconductor UNi_2Al_3. From the susceptibility we derive a crystalline-electric-field scheme, which closely resembles that of UPd_2Al_3. Furthermore, we examine the magnetic phase transition into the incommensurably ordered state at $T_N = 4.1$ K and construct the magnetic phase diagram for the three crystallographic directions. While for fields $\boldsymbol{B}$ parallel to the a- or c-axis T_N is monotonically lowered, this is not the case for $\boldsymbol{B}\|\boldsymbol{b}$. Instead, here we find a field-induced magnetic transition into a, presumably, commensurate ordered magnetic state. We discuss our results on UNi_2Al_3 in comparison to those for the related system UPd_2Al_3.

1. Introduction

In recent years heavy-fermion superconductors (HFS) attracted much attention due to the unusual superconducting and magnetic properties of these compounds. In particular, here the magnetic correlations could contribute to the coupling of the Cooper pairs, leading to unconventional types of superconductivity. Therefore, for HFS it is of special importance for achieving an understanding of the normal state and its magnetic properties in order to assess their influence on the superconductivity.

For one particular HFS, UPd_2Al_3 [1], it has been argued that the long-range magnetic ordering of the U ions does not play a role in the superconductivity [2]. Instead, similarly to the case of the magnetic superconductors [3], two subsets of f-electron systems should be present, one with a small mass enhancement carrying the antiferromagnetic ordering of large U moments of 0.85 μ_B below $T_N = 14.5$ K, and the other with heavy-fermion characteristics bearing the superconductivity below $T_c = 2$ K [1, 2, 4].

However, with this model it is difficult to explain why the closely related system UNi_2Al_3 exhibits a rather different behaviour with respect to its magnetic properties. This system undergoes a transition from a paramagnetic phase to an incommensurably ordered magnetic structure at $T_N = 4$ K, with U moments of 0.24 μ_B, while heavy-fermion superconductivity is observed at $T_c = 1$ K [5, 6]. It is not evident that the isoelectronic and isostructural systems UNi_2Al_3 and UPd_2Al_3 should behave so differently on a microscopic level as regards their magnetism, while the superconducting properties are qualitatively similar.

These issues are currently the focus of new experimental efforts, now that the first superconducting single crystals of UNi_2Al_3 have become available, yielding the opportunity to study the magnetic and superconducting anisotropies. Recently Sato *et al* [7] published

0953-8984/97/040913+10$19.50

the first data on the anisotropy of the superconducting properties of UNi_2Al_3. The magnetic bulk properties, however, they addressed only on a superficial level.

The magnetic anisotropies will be the subject of this report. We present susceptibility (χ_{dc}-) and resistivity (ρ-) data on the magnetic properties of superconducting single crystals of UNi_2Al_3. The anisotropy of the magnetic susceptibility we explain as arising from single-ion crystalline-electric-field (CEF) splitting. Furthermore, from the field dependence of the dc susceptibility and the resistivity we determine the magnetic phase diagram. In particular, we find a field-induced magnetic transition for fields $\boldsymbol{B}$ directed along the *b*-axis, and we argue that this is a transition from an incommensurably to a commensurably ordered state. We discuss our results in comparison with the magnetic properties of UPd_2Al_3 and their importance regarding the appearance of heavy-fermion superconductivity in UNi_2Al_3.

2. Experimental techniques

The single crystals investigated in this work were grown by use of a vertical floating-zone technique using a mirror-image furnace. Details regarding the growth and the characterization, including the superconducting properties, will be published elsewhere [8]. The crystals were annealed at 1000 °C for one week in high vacuum in quartz ampoules. Each crystal was checked by Laue diffraction for single crystallinity and alignment. In the following we denote as the *a*- and *c*-axes the conventional unit-cell vectors, while the term *b*-axis refers to a vector with indices $\langle 110 \rangle$, spanning an angle of 30° with the *a*-axis. The homogeneity of the crystals was checked by electron probe microanalysis. They were found to be single phase, and the composition was determined to be $UNi_{1.92\pm0.06}Al_{2.95\pm0.09}$.

The magnetic susceptibility was measured in a commercial SQUID, between 2 and 300 K in a field of 0.1 T, and at different fields up to 5 T between 2 and 6 K. The resistivity was obtained employing a conventional ac four-point technique, in zero magnetic field between 50 mK and 300 K, and in fields up to 8 T between 1.6 and 6 K.

The superconducting properties of the crystals were checked by means of ac resistivity measurements. For the two crystals cut along the *a*- and *b*-axis, superconducting transitions were observed at $T_c = 850$ mK with a typical transition width of 200 mK, while the transition for the crystal $\|\boldsymbol{c}$ was much broader with a width of about 500 mK.

3. Results

In figure 1 the overall magnetic susceptibility χ_{dc} and the normalized resistivity $\rho/\rho_{300\,\mathrm{K}}$ of UNi_2Al_3 are plotted for the three principal crystallographic directions. Due to unfavourable shapes of the crystals we could not determine accurately the resistivity of our crystals, though—as an estimate—the room temperature values of ρ are similar to those reported by Sato *et al* [7], i.e. about 150 $\mu\Omega$ cm.

For $\boldsymbol{B}\|\boldsymbol{a}$ and $\boldsymbol{B}\|\boldsymbol{b}$ the susceptibilities are nearly identical. For both directions we find a broad bump in χ_{dc} at about 100 K, while hardly any sign of a susceptibility bump is perceivable for $\boldsymbol{B}\|\boldsymbol{c}$. The resistivity exhibits common heavy-fermion behaviour with the downturn at low temperatures due to the depopulation of CEF and coherent scattering. There is some anisotropy to be seen in the resistivity between the *a*–*b* plane and the *c*-axis, but hardly any anisotropy can be noticed in the hexagonal plane. In the susceptibility a magnetic anomaly at $T_N = 4.1$ K (determined as the maximum in $\mathrm{d}(\chi_{dc}T)/\mathrm{d}T$ [9]) is visible for $\boldsymbol{B}\|\boldsymbol{a}$ and $\boldsymbol{B}\|\boldsymbol{b}$, which cannot be seen for $\boldsymbol{B}\|\boldsymbol{c}$. In contrast, for all three directions an anomaly at T_N can be observed in the resistivity. This is illustrated in figure 2, where we plot the

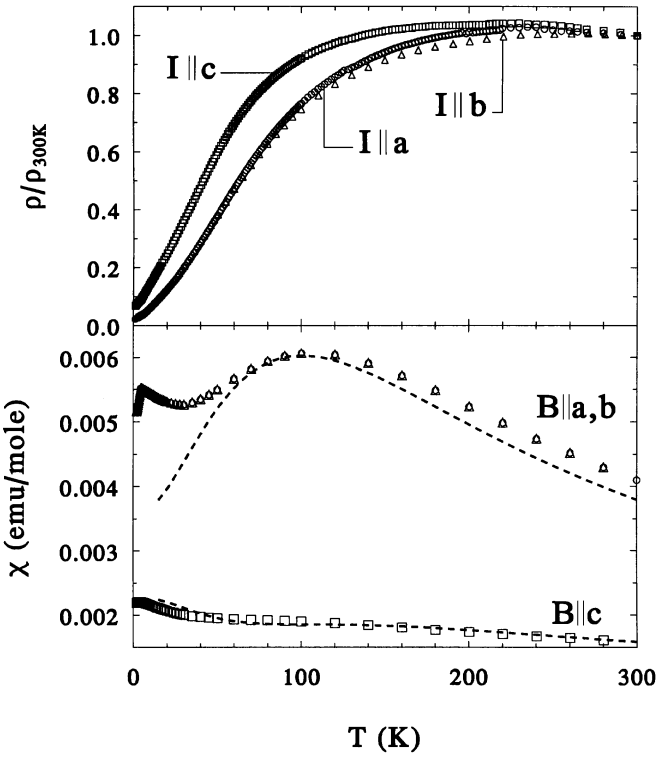

Figure 1. The dc susceptibility and the normalized resistivity of UNi_2Al_3 for the three principal crystallographic directions: $\boldsymbol{B}\|\boldsymbol{a}$ (○), $\boldsymbol{B}\|\boldsymbol{b}$ (△) and $\boldsymbol{B}\|\boldsymbol{c}$ (□). The dashed lines indicate the result of a calculation of the susceptibility using a crystalline-electric-field scheme as described in the text.

magnetic phase transition area of the resistivity for $\boldsymbol{I}\|\boldsymbol{a}$ and $\boldsymbol{I}\|\boldsymbol{b}$, as examples. The magnetic transitions are reflected in the resistivity by changes of slope, and the transition temperature T_N of UNi_2Al_3 (shown by Dalichaouch *et al* [10]) can be determined as minimum in the temperature derivative $\mathrm{d}\rho/\mathrm{d}T$ of the resistivity.

These results, in so far as they overlap, are in good agreement with those of Sato *et al* [7]. The anisotropy between the *a–b* plane and the *c*-axis with the maximum for $\boldsymbol{B}\|\boldsymbol{a}, \boldsymbol{b}$ qualitatively resembles the susceptibility anisotropy in UPd_2Al_3 [11]. For the latter system the susceptibility was interpreted in terms of CEF excitations from a singlet ground state, and could quantitatively be reproduced within a mean-field approach [11].

In analogy, we describe the susceptibility of UNi_2Al_3 in terms of CEF excitations. We follow the approach of Grauel *et al* [11], who assumed tetravalent U^{4+} ($5f^2$) as the uranium configuration in UPd_2Al_3. Starting from the crystalline-electric-field Hamiltonian in hexagonal symmetry

$$H_{eff} = H_{CEF} + H_{MF} = B_2^0 O_2^0 + B_4^0 O_4^0 + B_6^0 O_6^0 + B_6^6 O_6^6 + \lambda M \qquad (1)$$

and including a mean-field term λM, we can reproduce qualitatively and quantitatively the susceptibility of UNi_2Al_3 with the same tetravalent U configuration and a CEF scheme similar to that for UPd_2Al_3. The results of our calculation are indicated in figure 1 by the dashed lines. The level scheme qualitatively resembles the one proposed for UPd_2Al_3; it

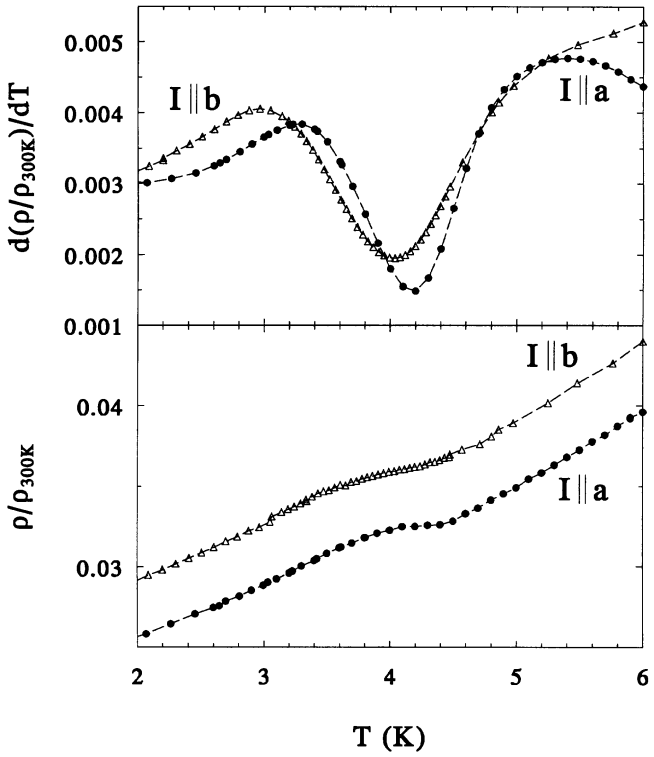

Figure 2. The magnetic phase transition of UNi_2Al_3, as seen in the resistivity for $\boldsymbol{I}\|\boldsymbol{a}$ and $\boldsymbol{I}\|\boldsymbol{b}$. T_N is determined as the minimum in $\mathrm{d}\rho/\mathrm{d}T$.

is only the energy splittings of the levels which we find to be larger by a factor of about 3 for the Ni compound than for UPd_2Al_3. The CEF scheme for UNi_2Al_3, thus, consists of a singlet ground state $|\Gamma_4\rangle$, an excited singlet $|\Gamma_1\rangle$ at 100 K, two excited doublets $|\Gamma_6\rangle$ and $|\Gamma_5\rangle$ at 340 and 450 K, another singlet $|\Gamma_3\rangle$ at 1300 K, and a doublet $|\Gamma_5\rangle$ at 1800 K, with a mean-field coefficient λ of -15 K (for a detailed account of the CEF calculations see Grauel *et al* [11] and Böhm *et al* [12]).

We regard our CEF analysis as evidence for a close relationship of the magnetic states of the two systems, UPd_2Al_3 and UNi_2Al_3. In the two compounds the basic magnetic anisotropies are similar, and they can be described by employing a comparable CEF picture. Only in UNi_2Al_3 is the level splitting larger than in UPd_2Al_3. On the basis of the CEF scheme and taking into account that the moment in U(Ni, Pd)$_2Al_3$ is an induced moment, we expect the ordered magnetic moment μ_{ord} and the magnetic transition temperature T_N of UNi_2Al_3 to be much smaller than for UPd_2Al_3, which is in agreement with the experimental findings [4, 6]. The two parameters, T_N and μ_{ord}, appear to be closely connected. With $\mu_{ord} \propto T_N$ and using UPd_2Al_3, $T_N = 14.5$ K and $\mu_{ord} = 0.85\ \mu_B$, we expect the ordered magnetic moment of UNi_2Al_3 to be, with $T_N = 4.1$ K, $\mu_{ord} = 0.24\ \mu_B$, in agreement with experiment [6].

Furthermore, we studied the field dependence of the magnetic transition temperature by resistivity and dc susceptibility measurements. In figure 3 we plot the field dependence of the normalized resistivity for the three principal directions. In figure 4 the field dependence

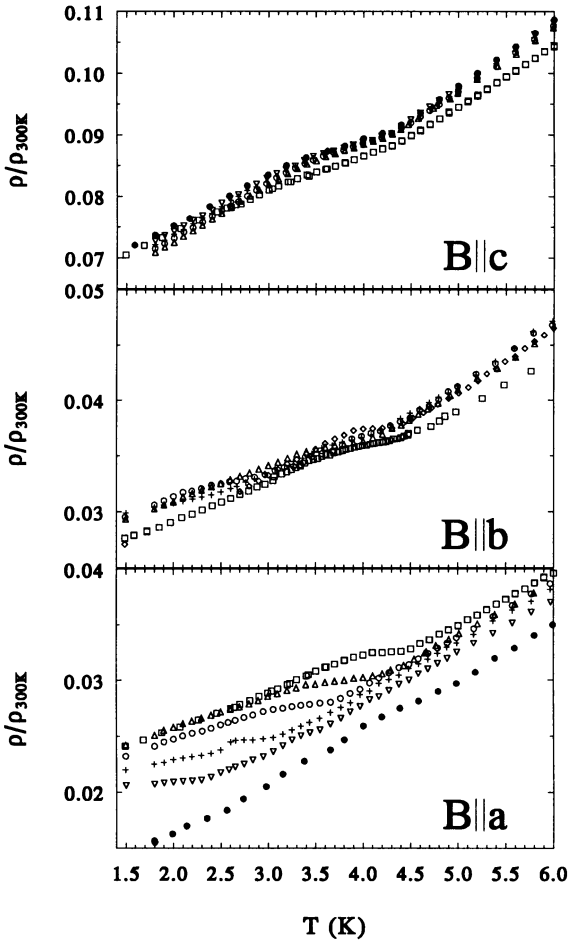

Figure 3. The magnetic anomaly in the resistivity of UNi_2Al_3 in different magnetic fields for the three principal crystallographic directions. The applied fields are 0 T (□), 1 T (◊), 3 T (△), 4 T (○), 5 T (+), 6 T (▽) and 8 T (●).

of the susceptibility for $\boldsymbol{B}\|\boldsymbol{a}$ and $\boldsymbol{B}\|\boldsymbol{b}$ is shown. From these plots it is obvious that the field dependences of the magnetic transition temperature—as of the measured properties in general—differ for the three principal directions.

The difference in behaviour for fields directed along the a- and the c-axis is similar to what is found for UPd_2Al_3 [11, 13]. While for $\boldsymbol{B}\|\boldsymbol{c}$ the decrease of T_N is weak, a much stronger decrease of T_N is found for $\boldsymbol{B}\|\boldsymbol{a}$. In contrast, the anomalous evolution of T_N for fields $\boldsymbol{B}$ directed along the b-axis is quite remarkable. For fields >3 T two kinks appear, and the resistivity susceptibility has two changes of slope. To illustrate this the two transitions are marked by the arrows in figure 4 for χ_{dc} at 4.5 T. And in figure 5 we plot the temperature derivatives of $\chi_{dc}T$ and $\rho/\rho_{300\,\mathrm{K}}$, both measured in 4.5 T for $\boldsymbol{B}\|\boldsymbol{b}$. The two anomalies observed in both derivatives suggest a field-induced magnetic transition in an intermediate-temperature regime. Since at both kinks in χ_{dc} the susceptibility drops as the temperature is lowered, such behaviour indicates antiferromagnetic coupling in both magnetic phases. Therefore, both transition temperatures can be determined as the maximum

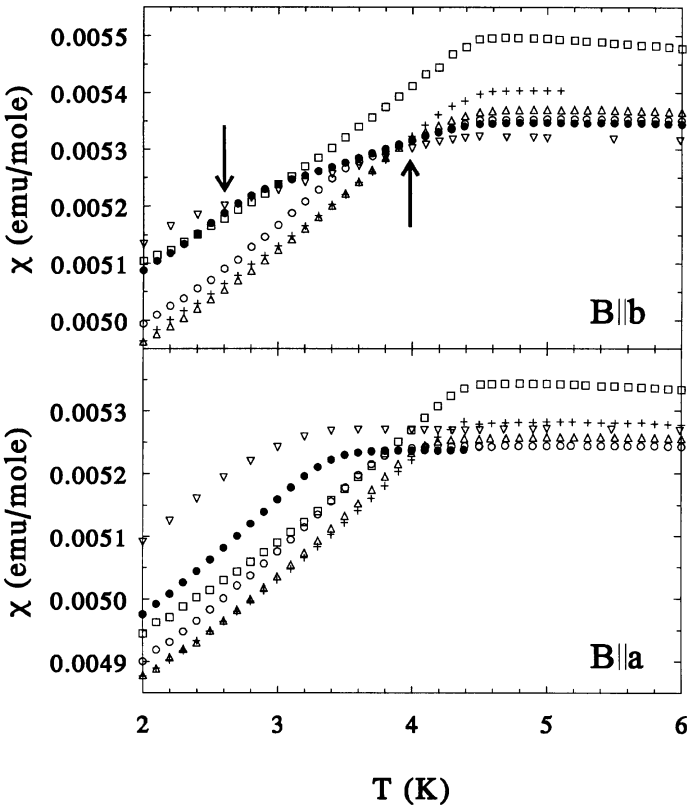

Figure 4. The magnetic anomaly in the susceptibility of UNi_2Al_3 for different magnetic fields directed along the *a*- and the *b*-axis. Measurements are taken at 0.5 T (□), 1.5 T (+), 2.5 T (△), 3.5 T (○), 4.5 T (●) and 5 T (▽). The arrows indicate the two transitions in the susceptibility for $\boldsymbol{B}\|\boldsymbol{b}$ at 4.5 T.

in $\mathrm{d}(\chi_{dc}T)/\mathrm{d}T$ and minimum in $\mathrm{d}\rho/\mathrm{d}T$, respectively.

From the anomalies in $\rho/\rho_{300\,\mathrm{K}}$ and χ_{dc} we can construct the magnetic phase diagrams for the three principal crystallographic directions. The three phase diagrams are displayed in figure 6. As mentioned above, we find pronounced differences for the three crystallographic directions. Although for $\boldsymbol{B}\|\boldsymbol{a}$ a smooth decrease of the phase borderline is seen, with T_N leaving our temperature window above 6 T, we only observe a decrease of T_N by 0.2 K for $\boldsymbol{B}\|\boldsymbol{c}$. On the other hand, for $\boldsymbol{B}\|\boldsymbol{b}$ we find three magnetic phases: (i) the incommensurably ordered phase I with a boundary similar to that determined for $\boldsymbol{B}\|\boldsymbol{a}$, but with smaller critical fields; (ii) a magnetic phase II, which is much more stable in high magnetic fields than phase I; and (iii) at higher temperatures the paramagnetic phase III.

4. Discussion

The wave vector of the incommensurate structure of UNi_2Al_3 was determined by Schröder *et al* [6] to be $\boldsymbol{q} = (\frac{1}{2} \pm \delta, 0, \frac{1}{2})$, $\delta = 0.110(3)$, with ordered moments of $\mu_{ord} = 0.24\ \mu_B$. This structure can be viewed as a longitudinal spin-density wave (LSDW) in the hexagonal plane, with the moments directed along the *b*-axis, and antiferromagnetic stacking of the

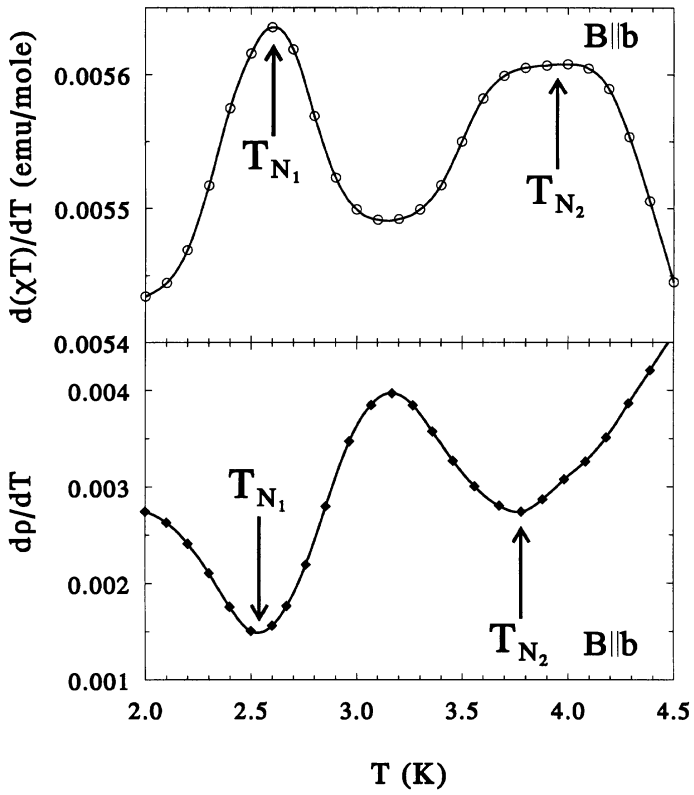

Figure 5. The temperature derivatives $\mathrm{d}(\chi_{dc}T)/\mathrm{d}T$ and $\mathrm{d}(\rho/\rho_{300\mathrm{K}})/\mathrm{d}T$ for $\boldsymbol{B}\|\boldsymbol{b}$ in a field of 4.5 T. The transition temperatures are determined as the maximum of $\mathrm{d}(\chi_{dc}T)/\mathrm{d}T$ and the minimum of $\mathrm{d}(\rho/\rho_{300\,\mathrm{K}})/\mathrm{d}T$.

moments along the c-axis. In UPd_2Al_3 the wave vector in the magnetically ordered state is commensurate, $\boldsymbol{q} = (0, 0, \frac{1}{2})$, implying that U moments of $\mu_{ord} = 0.85\ \mu_B$ are coupled ferromagnetically in the hexagonal plane and antiferromagnetically along the c-axis. Here, the easy magnetic axis is the a-axis [4].

We argue that the magnetic transition from phase I to phase II for $\boldsymbol{B}\|\boldsymbol{b}$ is one from the incommensurable state in UNi_2Al_3 with wave vector $\boldsymbol{q} = (\frac{1}{2} \pm \delta, 0, \frac{1}{2})$ to the commensurate one of UPd_2Al_3 with $\boldsymbol{q} = (0, 0, \frac{1}{2})$. Then, the ferromagnetic alignment of the moments in the hexagonal plane is stabilized. With the antiferromagnetic coupling along the c-axis two antiferromagnetically coupled sheets are rotated such that the spins lie perpendicularly with respect to the magnetic field, i.e. they point along the a-axis [14]. In contrast, this would be impossible for $\boldsymbol{B}\|\boldsymbol{a}$, and thus the magnetic field destroys the ordered state. In addition, fields directed along the c-axis can hardly affect the magnetically ordered state, which can be understood as arising from the single-ion anisotropy.

The different behaviours of the magnetically ordered state of UNi_2Al_3 for fields $\boldsymbol{B}$ oriented along the a- or b-axis implies that the basal-plane anisotropy energy is of a similar order of magnitude to the energy of the magnetic field at which the magnetic transition takes place. For $\boldsymbol{B}\|\boldsymbol{b}$, the contribution of the basal-plane anisotropy lowers the energy of the intermediate (commensurate) phase II both with respect to the paramagnetic phase III

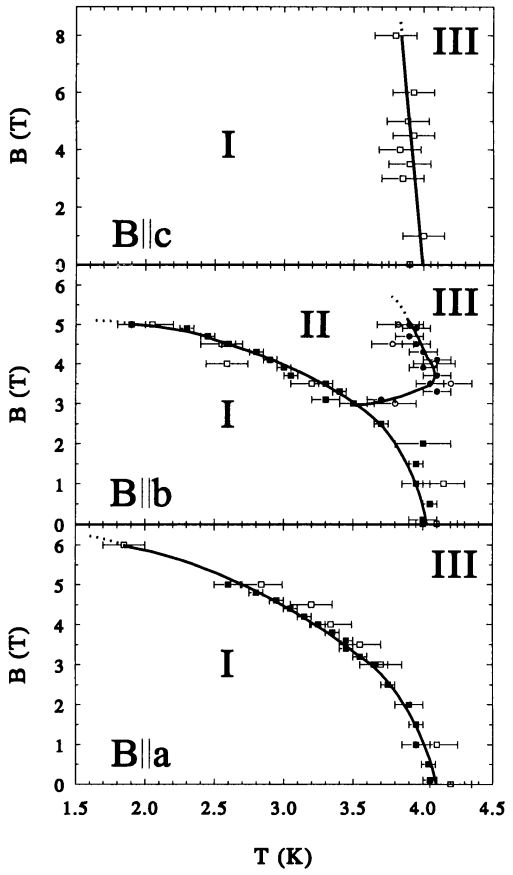

Figure 6. The magnetic phase diagrams of UNi_2Al_3 for the three principal crystallographic directions. Phase I is incommensurably ordered, phase II presumably commensurate and phase III paramagnetic. Filled data points have been derived from the susceptibility; open symbols indicate those determined via resistivity.

and the incommensurate phase I, while for $\boldsymbol{B}\|\boldsymbol{a}$ it increases the energy of phase II, thereby prohibiting a field-induced magnetic transition into II below 6 T. Now, since the magnetic field energy at the field-induced magnetic transition is rather small, it indicates that the basal-plane anisotropy energy is also comparably small. This again resembles the situation for UPd_2Al_3, where in torque measurements the basal-plane anisotropy energy was found to be small [14].

According to this scenario, the commensurate and incommensurate magnetic states in UNi_2Al_3 are energetically nearly degenerate. For near degeneracy there is no *a priori* reason for one of the two magnetic states to be the actual ground state. In other words, in this picture UNi_2Al_3 and UPd_2Al_3 appear as closely related as regards the magnetic properties. Only because of small differences in the band structures between the Pd and the Ni compounds is the magnetic ground state incommensurably ordered in UNi_2Al_3, while it is commensurate in UPd_2Al_3.

In conclusion, we have determined the anisotropy of the normal-state properties of UNi_2Al_3 for all three principal directions. We found that the bulk properties of UNi_2Al_3 can

consistently be described within a CEF picture, similarly to the case for previously studied UPd_2Al_3. From this scenario the quantitative differences of magnetic ordering temperatures and moments between UNi_2Al_3 and UPd_2Al_3 can be attributed to the larger CEF splitting in the Ni system, compared to the Pd compound. In particular, T_N and μ_{ord} seem to scale with each other. Furthermore, we have constructed the magnetic phase diagrams for the three crystallographic directions. A magnetic phase transition for $\boldsymbol{B}\|\boldsymbol{b}$ is found, and we argue that it indicates a transition from an incommensurable to a commensurable structure. Our results suggest a close relationship between the magnetic states of UNi_2Al_3 and UPd_2Al_3, removing the inconsistency regarding the magnetic properties of these chemically similar compounds. However, we are aware that, in order to definitely prove our interpretation, a neutron scattering experiment on single-crystalline UNi_2Al_3 in high magnetic fields should be performed.

In view of our results it is most interesting to briefly address the question of superconductivity in $U(Ni, Pd)_2Al_3$. Since in our model the magnetic and superconducting properties of $U(Ni, Pd)_2Al_3$ are basically similar, it implies that if the 2f-subsystem picture is valid for UPd_2Al_3, it should also apply to UNi_2Al_3. Here, it would be important to perform the investigations that have been interpreted as evidence for the 2f-subsystem picture in UPd_2Al_3 also on UNi_2Al_3. For instance, band-structure calculations for UNi_2Al_3 should lead to Fermi surfaces similar to those for UPd_2Al_3 [15–17]. Also, the experiments which have been explained within the 2f-subsystem model, like the pressure dependence of the specific heat [2] or spectroscopic experiments [18], should give similar results for UNi_2Al_3.

Another interesting possible study is that of the basal-plane anisotropy of the superconducting phase diagram. Our measurements prove the presence of basal-plane anisotropy of the magnetically ordered phase. If there is a coupling between superconductivity and the long-range magnetically ordered state, then this should be reflected in the anisotropic properties of the superconducting phase. Unfortunately, for the crystals used in this work, the superconducting transitions were too broad for us to obtain a reliable phase diagram of B_{c_2} in the hexagonal plane.

Acknowledgments

We would like to thank C C Mattheus and D Groten for assistance in the measurements. This work was partially supported by the Nederlandse Stichting voor Fundamenteel Onderzoek der Materie (FOM). The samples were prepared at FOM–ALMOS.

References

[1] Geibel C, Schank C, Thies S, Kitazawa H, Bredl C D, Böhm A, Rau M, Grauel A, Caspary R, Helfrich R, Ahlheim U, Weber G and Steglich F 1991 *Z. Phys.* B **84** 1

[2] Caspary R, Hellmann P, Keller M, Sparn G, Wassilew C, Köhler R, Geibel C, Schank C, Steglich F and Phillips N E 1993 *Phys. Rev. Lett.* **71** 2146

[3] See e.g.
Fischer Ø and Maple M B (ed) 1982 *Superconductivity in Ternary Compounds I* (Berlin: Springer)

[4] Krimmel A, Fischer P, Roessli B, Maletta H, Geibel C, Schank C, Grauel A, Loidl A and Steglich F 1992 *Z. Phys.* B **86** 161

[5] Geibel C, Thies S, Kaczorowski D, Mehner A, Grauel A, Seidel B, Ahlheim U, Helfrich R, Petersen K, Bredl C D and Steglich F 1991 *Z. Phys.* B **83** 305

[6] Schröder A, Lussier J G, Gaulin B D, Garrett J D, Buyers W J L, Rebelsky L and Shapiro S M 1994 *Phys. Rev. Lett.* **72** 136

[7] Sato N, Koga N and Komatsubara T 1996 *J. Phys. Soc. Japan* **65** 1555

[8] Mihalik M, Kayzel F E, Yoshida T, Kuwahara K, Amitsuka H, Sakakibara T, Menovsky A A and Franse J J M 1997 *SCES'96* submitted
[9] Fisher M 1965 *Lectures in Theoretical Physics* vol VIII C (Boulder, CO: University of Colorado Press)
[10] Dalichaouch Y, de Andrade M C and Maple M B 1992 *Phys. Rev.* B **46** 8671
[11] Grauel A, Böhm A, Fischer H, Geibel C, Köhler R, Modler R, Schank C, Steglich F, Weber G, Komatsubara T and Sato N 1992 *Phys. Rev.* B **46** 5818
[12] Böhm A, Grauel A, Sato N, Schank C, Geibel C, Komatsubara T, Weber G and Steglich F 1993 *Int. J. Mod. Phys.* **7** 34
[13] Oda K, Kumada T, Sugiyama K, Sato N, Komatsubara T and Date M 1994 *J. Phys. Soc. Japan* **63** 3115
[14] Süllow S, Janossy B, van Vliet G L E, Nieuwenhuys G J, Menovsky A A and Mydosh J A 1996 *J. Phys.: Condens. Matter* **8** 729
[15] Sticht J and Kübler J 1992 *Z. Phys.* B **87** 299
[16] Sandratskii L M, Kübler J, Zahn P and Mertig I 1994 *Phys. Rev.* B **49** 15 834
[17] Knöpfle K, Mavromaras A, Sandratskii L M and Kübler J 1996 *J. Phys.: Condens. Matter* **8** 901
[18] Takahashi T, Sato N, Yokoya T, Chainani A, Morimoto T and Komatsubara T 1996 *J. Phys. Soc. Japan* **65** 156